Constitutive modeling of anisotropy and microstructural evolution during superplastic deformation

F.K. Abu-Farha*

Mechanical Engineering Department & Center for Manufacturing, University of Kentucky, 151 Ralph G. Anderson Building, Lexington, KY 40506, USA

Abstract

In spite of continuously growing efforts and associated developments in the field of superplastic deformation, the limited predictive capabilities of deformation and failure remain a major obstacle that hampers the widespread use of the superplastic forming process. This work focuses on the development of an anisotropic microstructure-based constitutive model that can be used to accurately simulate the superplastic forming process. The model is capable of describing the superplastic deformation under simple tension and pure shear loading conditions.

Keywords: Superplasticity; Constitutive modeling; Anisotropy; Grain growth; Induced axial stresses; Simple tension; Simple shear

1. Introduction

Superplasticity is the phenomenon associated with certain classes of materials that have the ability to undergo very large uniform ductility. Superplastic forming (SPF) has been developed to utilize this phenomenon, and form various components from titanium, aluminum and other alloys for automotive and aerospace applications. SPF has many advantages over conventional forming processes; its ability to form very complicated geometries with cost and weight saving potentials. However, the industrial use of SPF is still limited to low volume applications, because of a number of issues that have been hampering its widespread use. One of the most important issues is the limited predictive capabilities due to lack of accurate constitutive models for superplastic deformation.

Significant efforts have been made to develop constitutive relations that describe the superplastic deformation, but most of these efforts are based on the uniaxial loading condition and/or assume isotropic behavior. In addition, only few models take the effect of microstructural evolution on the deformation into account [1,2,3,4]. However, studying the deformation under uniaxial loading condition does not give any insight on possible directional effects that may result from an anisotropic structure. Recent multiaxial experiments on the Pb-Sn superplastic alloy have showed a strong degree of deformation-induced anisotropy and transient behavior, which can be associated with development of internal (*back*) stresses [5,6].

In this work, we present a generalized microstructure-based multiaxial constitutive model that can describe the anisotropic superplastic deformation. The focus will be on the anisotropic and microstructural aspects of the model. The developed model is simplified to the uniaxial and simple shear loading cases, and the predicted stresses are compared with the experimental data. It is shown that the model can accurately capture the material behavior for the two loading cases, in addition to the induced axial stresses measured in fixed-end torsion test.

2. Constitutive model

On the basis of the continuum theory of viscoplasticity with internal variables, the general associated flow rule for superplastic deformation is given by the following tensor equation [7,8]:

$$D_{ij} = f\frac{\partial J}{\partial \sigma_{ij}} = \left[\frac{C_i(J-(K_0+R))^{\frac{1}{m}}}{d^p} + C_{ii}J^n\right]\frac{\partial J}{\partial \sigma_{ij}} \qquad (1)$$

* Tel.: +1 (859) 257 6336; Fax: +1 (859) 323 1039; E-mail: rurouni@engr.uky.edu

Computational Fluid and Solid Mechanics 2005
K.J. Bathe (Editor)

where D_{ij} is the rate of deformation tensor, f is the overstress function, $J(\sigma_{ij} - \alpha_{ij})$ is the anisotropic yield function, σ_{ij} and α_{ij} are the Cauchy and internal stress tensors, respectively, R is the isotropic hardening, m is the strain rate sensitivity index, n is the stress exponent, d is the average grain diameter, p is the grain growth exponent, and C_i, C_{ii} and K_0 are material parameters.

Equation (1) accounts for microstructural evolution and the internal variables if these variables are updated during deformation; this can be achieved by introducing the evolution equations.

2.1. Grain growth equation

A grain growth model similar to the one used by Johnson et al. [9] will be used here, by combining both static and dynamic parts. The rate equation has the following form:

$$\dot{d} = \dot{d}_S + \dot{d}_D = \frac{k_s}{d^g} + \frac{k_d \tau \dot{\varepsilon}}{d^g}\left(1 - \exp\left(\frac{-t}{\tau}\right)\right) \tag{2}$$

where t is time, and k_s, g, k_d and τ are material constants.

2.2. Evolution equations of internal variables

Equation (1) includes a set of internal variables: back stress α, isotropic hardening R and the anisotropic angle ϕ. The evolution equations for these internal variables are consistent with those used in viscoplasticity and include hardening, dynamic recovery, and static recovery terms:

$$\dot{R} = H\dot{\bar{\varepsilon}} - C_D\dot{\bar{\varepsilon}}R - C_S R^a \tag{3}$$

$$\overset{\circ}{\alpha} = HD - C_D\dot{\bar{\varepsilon}}\alpha - C_S\alpha(h(\alpha))^{a-1} \tag{4}$$

where H, C_D and C_S are the hardening, dynamic recovery and static recovery coefficients, and a is the static recovery exponent; $h(\alpha)$ has the form of the anisotropic yield function, where $h(\alpha) = J(\alpha)$.

Motivated by the work of Dafalias [10], the evolution of ϕ is given by:

$$\dot{\phi} = -\frac{\sqrt{3}\dot{\bar{\varepsilon}}}{2}\left[x(1 - \xi(\alpha_{11} - \alpha_{22})) + (1 - x)(1 - \eta\cos(2\phi))\right] \tag{5}$$

where $\dot{\bar{\varepsilon}}$ is the effective strain rate, and x, ξ and η are material parameters.

2.3. Anisotropic yield function

To capture the anisotropic behavior during deformation, a generalized anisotropic yield function is used here [7,8]:

$$J = \begin{bmatrix} \frac{3}{2}\left(S_{ij} - \alpha_{ij}\right)\cdot\left(S_{ij} - \alpha_{ij}\right) + c_1\left[M_{ij}\cdot\left(S_{ij} - \alpha_{ij}\right)\right]^2 + \\ c_2\left[N_{1ij}\cdot\left(S_{ij} - \alpha_{ij}\right)\right]^2 + c_3\left[N_{2ij}\cdot\left(S_{ij} - \alpha_{ij}\right)\right]^2 \end{bmatrix}^{\frac{1}{2}} \tag{6}$$

where S_{ij} is the deviatoric stress tensor, M_{ij}, N_{1ij} and N_{2ij} are directional tensors expressed in terms of ϕ [8], and c_1, c_2 and c_3 are the anisotropic constants (*for* $c_1 = c_2 = c_3 = 0$, *the anisotropic yield function reduces to the isotropic von Mises one*).

2.4. Solution

Equation (1) is a tensor equation that represents a total of six equations for the six independent stress and strain rate components. Yet, for any particular loading case, the equation can be reduced to a certain number (*usually lesser*) of independent equations; each relates a strain rate component to the associated stress component. The same applies to the back stress tensor in Eq. (4).

For the given strain rate/s, the grain growth and the evolution equations are first solved, and along with Eq. (6), are fed into the constitutive model reduced from Eq. (1). The constitutive model is solved for the stress component/s corresponding to the given strain rate/s.

3. Results

The general constitutive model was reduced to both simple tension and pure shear loading conditions, in order to calibrate the model and fit the experimental data. The different material parameters in the previous equations were determined from a number of tests conducted on the model Pb-Sn superplastic alloy [7].

3.1. Simple tension

Since there is one stress component (σ_{11}) associated with uniaxial loading case, the tensor Eq. (1) reduces to one equation that relates ϵ_{11} to σ_{11}:

$$\dot{\varepsilon}_{11} = \left[\frac{C_i[J - (K_0 + R)]^{\frac{1}{m}}}{d^p} + C_{ii}J^n\right]\frac{\partial J}{\partial \sigma_{11}} \tag{7}$$

A plot of the predicted axial stresses compared to the experimental data at different strain rates is shown in Fig. 1. The model is capable of describing the superplastic behavior of the material by capturing its strain rate sensitivity and the hardening/softening behaviors. The effect of anisotropy on the predicted stresses was observed to be insignificant, which is expected, as the uniaxial loading does not give any insight on possible directional effects caused by an anisotropic structure. On

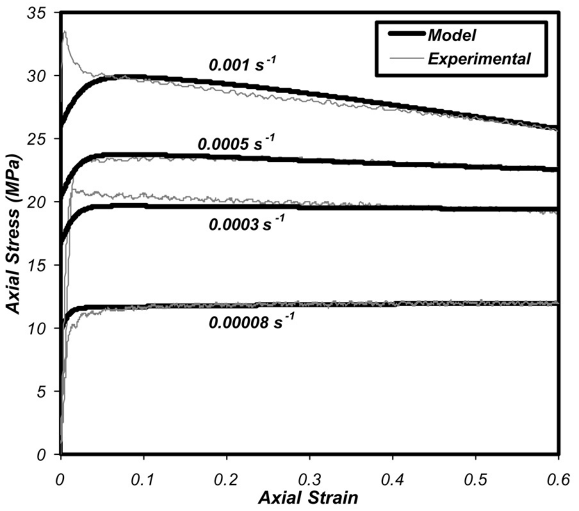

Fig. 1. Predicted and experimentally constructed stress–strain curves in simple tension.

the other hand, the effect of grain growth was proven significant, as it is clearly depicted from Fig. 2. Incorporating grain growth into the constitutive model allows it to capture the appropriate softening and hardening behaviors at different strain rates.

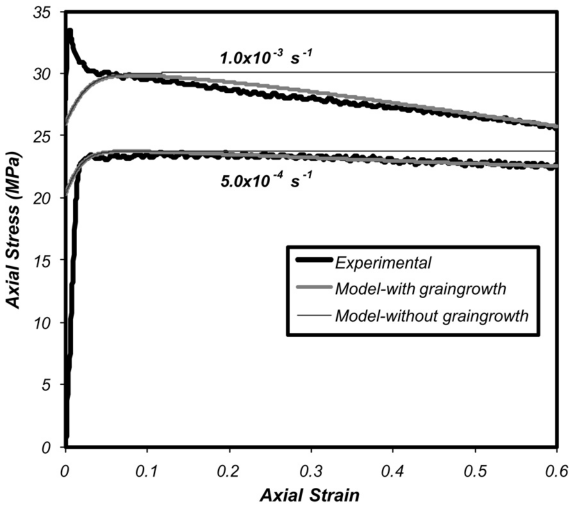

Fig. 2. Effect of grain growth on the axial stresses in simple tension.

3.2. Pure shear

A simple shear loading case is simulated by a pure torsion test. But since anisotropy is taken into account, induced axial stresses/strains are expected depending on the type of test performed. For a fixed-end torsion test, induced axial stresses appear in the stress tensor as additional axial stress components, without affecting the rate of deformation tensor. Consequently, Eq. (1) becomes:

$$\mathbf{D}_{11} = 0 = \left[\frac{C_i(J-(K_o+R))^{\frac{1}{m}}}{d^p} + C_{ii}J^n \right] \frac{\partial J}{\partial \sigma_{11}} \tag{8}$$

$$\mathbf{D}_{12} = \frac{\dot{\gamma}}{2} = \left[\frac{C_i(J-(K_o+R))^{\frac{1}{m}}}{d^p} + C_{ii}J^n \right] \frac{\partial J}{\partial \tau_{12}} \tag{9}$$

$$\mathbf{D}_{22} = 0 = \left[\frac{C_i(J-(K_o+R))^{\frac{1}{m}}}{d^p} + C_{ii}J^n \right] \frac{\partial J}{\partial \sigma_{22}} \tag{10}$$

Similarly, the model successfully captures the surface shear stresses measured in fixed-end torsion tests at different strain rates, as shown in Fig. 3. In addition, the model with the employed anisotropic yield function predicts the development of induced axial stresses, as shown in Fig. 4. These induced stresses are indicative of deformation-induced anisotropy, and follow the actual trend of the experimentally recorded ones [8]. Capturing these stresses was not feasible with an isotropic yield function [7].

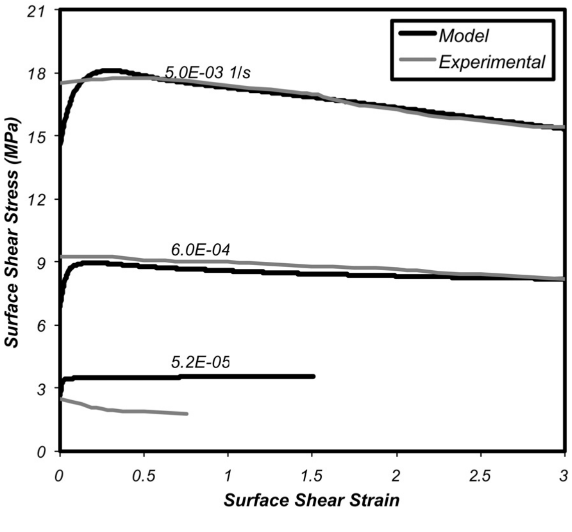

Fig. 3. Predicted and experimentally constructed shear stress–strain curves in simple shear.

4. Conclusions

A multiaxial constitutive model for superplastic deformation, which accounts for grain growth, anisotropy and the evolution of internal variables, was presented. The model was reduced to the uniaxial and

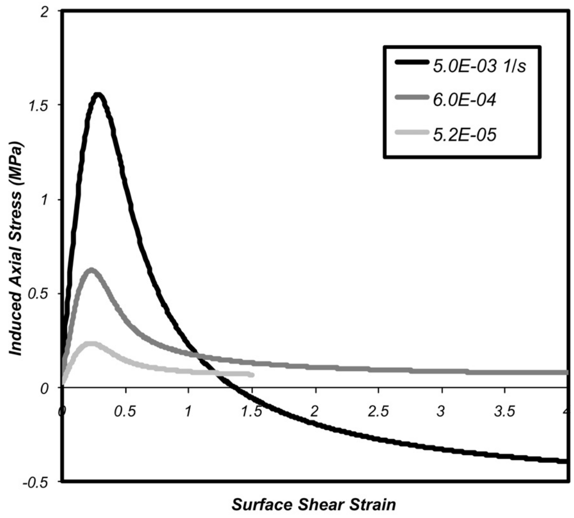

Fig. 4. Predicted induced axial stresses in fixed-end torsion.

pure shear loading cases, where it successfully captured the experimentally observed superplastic behavior of the model material.

Grain growth effect was clearly shown in simple tension, where the model captured the hardening/softening behavior at different strain rates. Anisotropy had no significant effect in simple tension; however, it enabled the model to predict the induced axial stresses observed in fixed-end torsion.

Acknowledgment

I would like to acknowledge my advisor Dr. Marwan Khraisheh.

References

[1] Hamilton C, Zbib H, Johnson C, Richter S. Dynamic grain coarsening, its effects on flow localization in superplastic deformation. In: Proc. of 2nd SAMPE Symposium, Chipa, Japan, 1991, pp. 272–279.

[2] Davies G, Edington J, Cutler C, Padmanabhan K. Superplasticity: a review. J Mat Sci 1970;5:1091–1102.

[3] Dutta A, Mukherjee M. Superplastic forming: an analytical approach. Materials science and engineering 1992;A157:9–13.

[4] Carrino L, Guiliano G. Modeling of superplastic blow forming. Int J Mech Sci 1997;39:193–199.

[5] Zhang K, Hamilton C, Zbib H, Khraisheh M. Observation of transient effects in superplastic deformation of Pb-Sn eutectic alloy. Scripta Metall Mat 1995;32(6):919–923.

[6] Khraisheh M, Bayoumi A, Hamilton C, Zbib H, Zhang K. Experimental observation of induced anisotropy during the torsion of superplastic Pb-Sn eutictic alloy. Scripta Metall Mat 1995;32(7):955–959.

[7] Khraisheh M, Zbib H, Hamilton C, Bayoumi A. Constitutive modeling of superplastic deformation, part I: theory and experiments. Int J Plasticity 1997;13(1/2):143–164.

[8] Abu-Farha F, Khraisheh M. Constitutive modeling of deformation-induced anisotropy in superplastic materials. Mat Sci Forum 2004;447–448:165–170.

[9] Johnson C, Hamilton C, Zbib H, Richter S. Designing optimized deformation paths for superplastic Ti6Al4V. Adv Superplasticity Superplastic Forming 1993;3–15.

[10] Dafalias Y. The plastic spin in viscoplasticity. Int J Solids Struct 1990;26:149–163.